

Electrochemical Properties and XPS Analysis of Ni-B/SiC Nanocomposite Coatings

Weiwei Zhang^{1,*}, Baosong Li^{2,*}

¹ College of Mechanical and Electrical Engineering, Hohai University, Changzhou 213022, China

² College of Mechanics and Materials, Hohai University, Nanjing 211100, China

*E-mail: zdzdq@126.com, lbs79@126.com

Received: 17 December 2017 / *Accepted:* 30 January 2018 / *Published:* 6 March 2018

Few studies have reported the electrochemical properties and XPS analysis of Ni-B/SiC nanocomposite coatings with high wear resistance prepared by electro-co-deposition. In this study, Ni-B/SiC nanocomposite coating was prepared by electrodeposition using trimethylamine borane as boron source in a Ni-B electrolyte containing dispersed SiC nanoparticles. The corrosion resistance and anti-wear properties of the Ni-B/SiC composite coating were examined. XPS was employed to analyze the element electronic state of the coating surface. The results show that the corrosion resistance of the Ni-B/SiC composite coating was enhanced which may be related to the dense structure, barrier effect and the reduction in the active surface area of Ni-B matrix by the presence of inert SiC particles. The XPS analysis indicated that the as-deposited coating contains metallic nickel, oxide or hydroxide nickel, and the SiC particles. Ni-B/SiC nanocomposite coating with dense structure shows superior anti-corrosion and wear resistance than Ni-B and Ni/SiC coatings.

Keywords: Electrodeposition; Ni-B/SiC nanocomposite coating; wear resistance; corrosion resistance; microhardness

1. INTRODUCTION

A variety of techniques, such as physical vapor deposition, chemical vapor deposition, ion implantation, sputtering in vacuum, are available for the preparation of Ni-B composite coatings. Nevertheless, the electro- and electroless plating processes are still widely employed due to their low production cost, industrial capability, easy implementation, size and shape flexibility, and high production rates [1-3]. Literatures are available on the synthesis and characterization of electroless Ni-B coatings [4, 5]. Electroless deposition is a representative method of forming Ni-B coatings [6]. However, as a rule, electroless deposition is operated at high temperature (70-90°C) and high pH

values (13-14) [7], in which process strict control of pH is essential [8]. Ni-B alloy coatings can also be deposited electrochemically from the baths containing dimethylamine borane [9], trimethylamine borane [8], and sodium decahydroclovodecaborate [10]. Compared with the electroless method, the electrochemical technique offers several advantages, such as high growing rate, low bath temperature, good stability, ease control and uniform distribution of boron in the coating. However, up to now, very limited reports are available on the synthesis of Ni-B composite coatings through electrodeposition [11, 12]. Also, the Ni-B alloy may not possess all the necessary properties in special applications [13]. Therefore, Ni-B composite coatings reinforced by nanoparticles via co-deposition is gaining increasing attention.

Ni-B/SiC nanoparticles is a hard and wear resistant coating due to their good thermal stability, high hardness, wear resistance and corrosion resistance [14, 15]. Ogihara et al. [16] reported that Ni-B/SiC composite coatings could be electrodeposited using trimethylamine borane as boron source, which showed superior mechanical properties to Ni/SiC and Ni-P/SiC composite coating. Georgiza et al. [17] reported that incorporation of SiC in Ni-B alloy was obtained in the presence of surfactant tween 20 by electroless plating. They found that the hardness of the coating was greatly increased and the embedded SiC particles reduce the metallic area prone to corrosion. Bekish et al. [10] examined the relationship between corrosion resistance and structure of electrodeposited Ni-B films and concluded that the corrosion resistance of the nanocrystalline Ni-B coatings is essentially higher than that of the amorphous ones.

Until now, the electrochemical properties and wear resistance of the Ni-B/SiC composite coatings prepared by electrodeposition have rarely been reported [18]. Moreover, it is necessary to investigate the surface element electronic state of the coating through XPS analysis. In this study, we prepared Ni-B/SiC composite coatings by electrodeposition. The main objective was to elucidate the corrosion resistance, anti-wear properties and XPS analysis of the electrodeposited Ni-B/SiC composite coatings. New data on the electrochemical and XPS properties of the Ni-B/SiC composite coatings deposited in an electrolyte containing trimethylamine borane were obtained.

2. EXPERIMENTAL

Ni-B/SiC composite coatings were prepared by electrodeposition from a typical Watt's Ni bath containing trimethylamine borane as boron source. The bath composition and operating parameters are listed in Table 1. Analytical reagents and deionized water were used to prepare the plating solution. The Cu substrates were masked with insulated tapes to leave 20×20 mm² of the exposed area. A nickel plate was used as counter electrode. The Cu and Ni plates were positioned vertically in a 200 ml electrodeposition baths. The distance between the Cu and Ni was fixed around 25 mm. The average size of the as-received SiC particles (purity >99.9%) was ≤150 nm. The electrolytes were stirred for 24 h just before electrodeposition to obtain de-agglomerated particles. The electrodeposition current densities were varied from 0.5 to 7 A dm⁻², SiC particles 2.5 to 12.5 g L⁻¹, and TMAB 0 to 9 g L⁻¹. In the experiment, only varies the one investigated parameter and the other parameters are still the same to Table 1. The pH values of the baths were adjusted to 3.5 using H₂SO₄ or NiCO₃. Thermal treatment

was conducted in an electric furnace that had been heated to 200 to 600 °C in air, and kept at that temperature for 1 h.

Table 1. Bath composition and operating parameters for Ni-B/SiC composite coatings.

Electrolyte composition		Electrodeposition parameters	
NiSO ₄ ·6H ₂ O	200 g/L	pH	3.5
NiCl ₂ ·6H ₂ O	50 g/L	Temperature	45 °C
H ₃ BO ₃	30 g/L	Current density	0.5- 7 A·dm ⁻²
Trimethylamine borane(TMAB)	3 g/L	Agitation rate	450 ± 50 rpm
Sodium dodecyl sulfate(SDS)	0.5 g/L	Electrode distance	2.5cm
Saccharine	1 g/L	Deposition time	15-90 min
SiC nanoparticles	0-15 g/L	Anode	Ni plates

XPS was collected by a Thermo ESCALAB 250Xi spectrometer using unmonochromatized Al K α radiation (1486.6 eV) to analyze the surface element electronic state of the coating. The wear resistance of specimens was evaluated on UMT-3 multi-function friction and wear tester with a ball-on-disc configuration. Counterparts were SiC balls with a diameter of 3 mm and a hardness of 17 GPa. Wear tests were carried out with a frequency of 5 Hz and amplitude of 2.5 mm under 10 N for dry-sliding. Each specimen was tested three times under the same condition to collect an average value. A surface profiler (Alpha-Step IQ) was used to measure the wear track profile. The corrosion behavior of the Ni-B/SiC composite coating was evaluated in a conventional three-electrode cell with a saturated calomel electrode (SCE) as a reference electrode and platinum as an auxiliary electrode. The samples were embedded in an epoxy resin, leaving an area of 1 cm² exposed as the working electrodes. The measurements were conducted in 3.5% NaCl solution without agitation at 25 °C using a potentiostat (CHI 660E). The bath was deoxidized 20 min by Nitrogen before electrodeposition. The electrochemical impedance spectroscopy (EIS) was carried out, referring to a frequency range of 10⁻²-10⁵ Hz and amplitude 10 mV. The Tafel curves of the electrolyte were recorded at a sweep rate of 1 mV/s in 3.5% NaCl solution at room temperature.

3. RESULTS AND DISCUSSION

3.1 Corrosion resistance of Ni-B/SiC composite coatings

Few works have studied the corrosion properties of Ni-B matrix containing SiC nanoparticles. Fig. 1 shows the potentiodynamic polarization curves of the Ni-B/SiC prepared at different conditions after immersed in 3.5% NaCl solution for 1 day and 20 days. It can be seen in Fig. 1(a) that, with the increase of TMAB concentration in the plating bath, the E_{corr} of the Ni-B/SiC coating shifts to the negative potential. This indicates that the inclusion of B is not necessary to improve the corrosion resistance of the coating. Fig. 1(a) also shows that i_{corr} slightly increases with the increase of the TMAB concentration. It is probably because that with the increase of the boron content in the

composite coating, the brittle fracture will be promoted for the Ni-B matrix with a high content of boron in the coating, which will deteriorate the corrosion resistance of the coating. Another reason is related to the high internal stress in the deposits due to the intense hydrogen evolution reaction. The high content of boron in the coating has deleterious effects on the corrosion properties. After immersed in 3.5% NaCl solution for 20 days, the same results were found to that of 1 day through the E_{corr} decreases and i_{corr} increases correspondingly. As shown in Fig. 1(b), the addition of SiC particles have reduced the i_{corr} of the Ni-B/SiC coating though no obvious variation of E_{corr} was found. This indicates that the incorporation of SiC particles enhances the corrosion resistance of the Ni-B coating. This improvement in corrosion resistance was attributed to the reduction in the active area of Ni-B matrix by the inclusion of inert SiC particles. After immersed 20 days in 3.5% NaCl solution, it was found that the coating with 5 gL^{-1} SiC particles has better corrosion resistance.

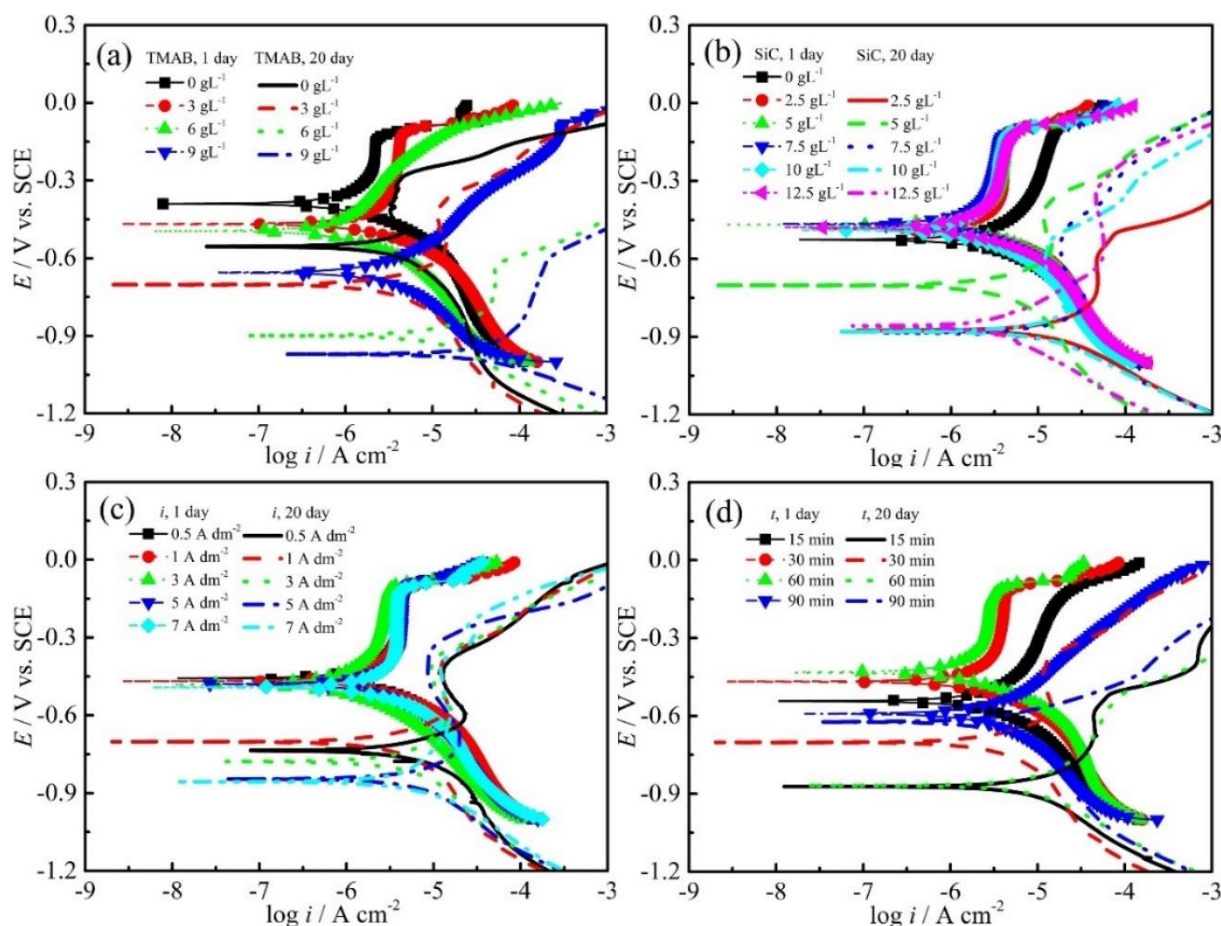


Figure 1. Tafel curves of Ni-B/SiC composite coatings electrodeposited with different (a) TMAB concentrations; (b) SiC concentrations; (c) current density; (d) deposition time after immersed in 3.5 wt.% NaCl solution for 1 day and 20 days. Other parameters: TMAB 3 gL^{-1} , SiC 5 gL^{-1} , $1 \text{ A} \cdot \text{dm}^{-2}$, 30 min, pH 3.5, expect for the one investigated (varied) parameter.

Fig. 1(c) shows that by increasing the current density from 0.5 to 1 A dm^{-2} , the E_{corr} of the Ni-B/SiC coating shifts to the positive potential, and the i_{corr} decreases at the same time, which is an indicator of the improvement of corrosion resistance. Noted that the same deposition time (30 min)

was employed in this section. Therefore, the coating obtained at different current density has the different thickness which also means the different growth rate. The thickness of the coating obtained at low current density is smaller than that prepared at the high current density under the same deposition time. Thus, the Fig. 1(c) describes the coatings with the different thickness which prepared at different current density. So, it could not directly elucidate the effects of current density on the properties of the coatings under the extra effects of the thickness. Fig. 1(c) still shows that the coatings deposited at 1 A dm^{-2} has better corrosion resistance after immersed for 20 days in 3.5% NaCl solution. With the extending of electrodeposition time, the coating became thicker which is beneficial to the improvement of corrosion resistance via physical shielding. Nevertheless, the coating will become darker or greyish, and serious cracks will emerge when continuously electrodeposition for more than 90 min, which has detrimental effects on the anti-corrosion performance. Fig. 1(d) shows that the Ni-B/SiC coatings deposited 30 min have the lower i_{corr} and high E_{corr} value, which is an indication of better corrosion resistance and stability.

Fig. 2 shows the Nyquist plots of the Ni-B/SiC prepared at different conditions after immersed in 3.5% NaCl solution for 24 h. As can be seen in Fig. 2(a), the addition of 3 g L^{-1} TMAB have a beneficial effect on the improvement of the anti-corrosion properties of the Ni-B/SiC composites. It also indicates that more or less than 3 g L^{-1} TMAB will decrease the corrosion resistance of the coating. This is associated with the high internal stress and brittle fracture with high B content in the coating. It is known that additional capacitance character can improve the protective ability of the coating through hindering substance transportation across the coating. The Ni-B coatings with a low boron content show better corrosion resistance which may be due to the grain refinement compared to boron-free ones. The corrosion resistance will be enhanced significantly as the grain size refined to nanocrystalline. This is related that the more rapid formation of a compact protective oxide film on nanocrystalline Ni surface due to a higher density of nucleation sites for the passive film.

As shown in Fig. 2(b), when current density was 0.5 and 1 A dm^{-2} , the R_p of Ni-B/SiC was small compared to other samples. Increasing the current density to 5 A dm^{-2} , the R_p sharply increases to the maximum. However, continue to increase the current density to 7 A dm^{-2} , the R_p decreases again. As for the 7 A dm^{-2} , considering that the same deposition time was adopted which results in the different coating thickness, it can be concluded that the corrosion resistance begins to deteriorate when current density exceeds 5 A dm^{-2} .

Fig. 2(c) indicated that with the increase of the SiC concentration, the R_p increases which indicates the increase of the corrosion resistance of the composite coating. Then, when SiC particles surpass 10 g L^{-1} , the decrease of R_p was observed. The R_p of Ni-B/SiC composite coatings prepared in 10 g L^{-1} SiC in the solution is larger than that of Ni-B alloy and other composites which shows that they have superior corrosion resistance. It was already discussed that the presence of inert SiC particle could reduce the active area of Ni-B matrix. Furthermore, the identical shapes of the Nyquist plots indicate that the corrosion mechanism of the coating is invariant and the solution has not reached the substrate through the coating. The inclusion of SiC inhibits the matrix dissolution and, consequently, significantly enhances the coating corrosion resistance. In composite coatings, SiC can fill the surface defects, acting as a barrier and hindering the corrosion attack. On the other hand, grain refinement also

improves the corrosion resistance of the composite coating. Thus, the corrosion resistance is also complementarily strengthened by incorporation of SiC particles into Ni-B matrix coating.

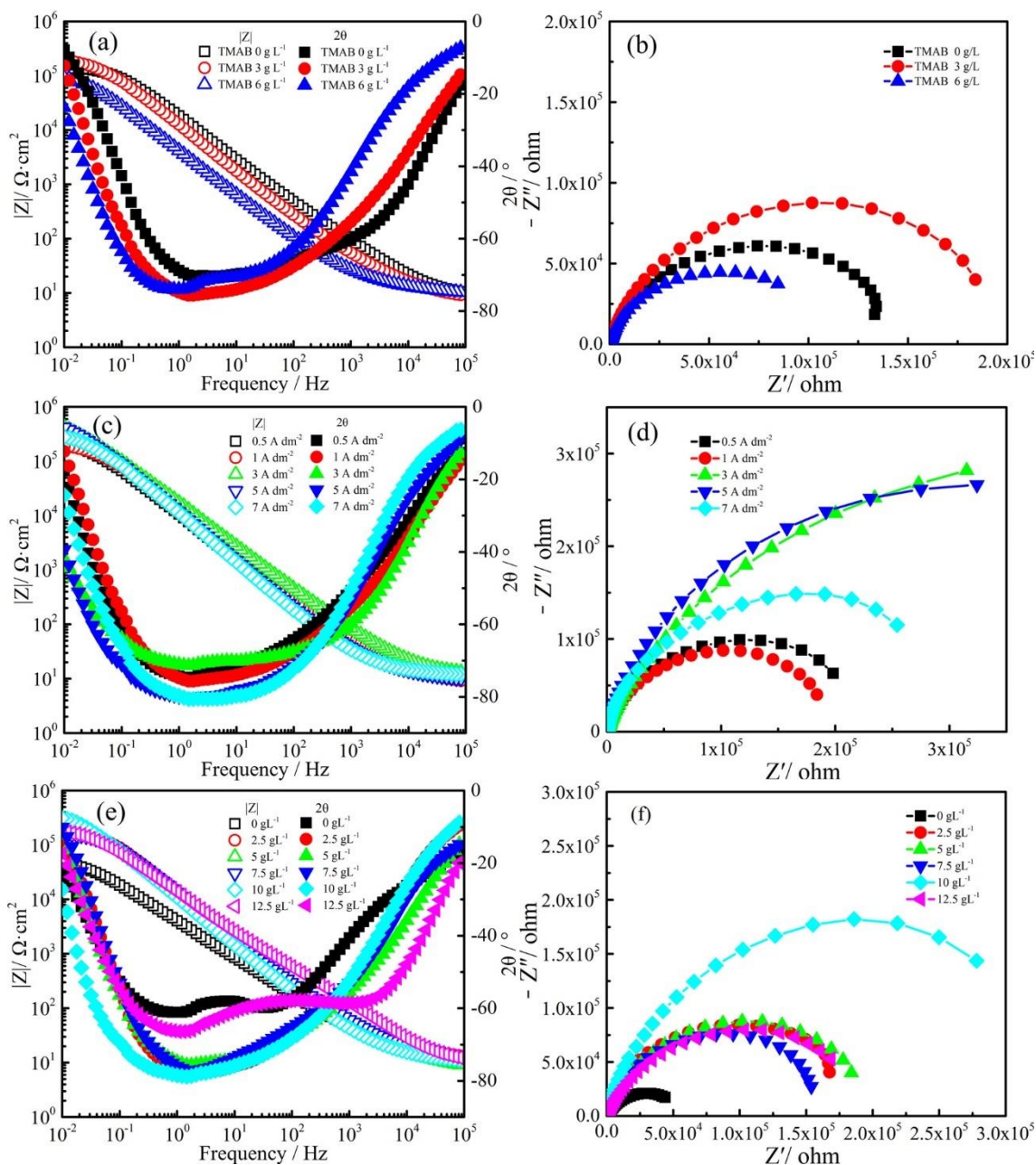


Figure 2. Nyquist diagrams and bode plots of Ni-B/SiC composite coatings electrodeposited with different (a, b) TMAB concentrations; (c, d) current density; (e, f) SiC concentrations after immersion for 24 h in 3.5 wt.% NaCl solution. Except for the one investigated (varied) parameter, other parameters are the same to Table 1.

3.2 Wear resistance of Ni-B/SiC nanocomposite coatings

Fig. 3 comparatively shows the friction coefficient of different coatings under dry-sliding condition (10 N, 5 Hz). Fig. 3(a) shows that the stable friction coefficient of the Ni-SiC coating is

about 0.35. With the incorporation of B into the Ni-SiC coatings, the friction coefficient increases from 0.38 up to 0.4, 0.43 corresponding to the TMAB concentration of 3, 6 and 9 g L⁻¹, respectively. Fig.3 (c) shows that the friction coefficient of the Ni-B/SiC is between 0.63 and 0.67 when the current density is 3 A dm⁻². At 5 A dm⁻², the friction coefficient increases to 0.69. As a result, the value of the friction coefficient is affected by the B content and current density of the electrodeposition. The wear track profiles is an intuitive way to compare the wear rates of different coatings. The wear track profiles were measured using a surface profiler (Alpha-Step IQ). Origin 9 software is used to calculate area size of the wear track profile. The wear rates of specimens were calculated using the equation: $A=V/F \cdot L$, where V is the wear volume loss (mm³), L is the total sliding distance (m), and F is the normal load (N). Under the dry-sliding condition (10 N, 5 Hz), the wear rate of as-deposited Ni-B/SiC coatings is between 0.45×10^{-6} to 2.21×10^{-6} mm³/Nm when bath contains 3 g L⁻¹ TMAB, 5 g L⁻¹ SiC particles. However, as for the coatings of Ni/SiC or Ni-B, it was found that the wear rate was extremely high in comparison with Ni-B/SiC composite coating. The Ni-B/SiC composite coating exhibits better wear resistance than that of Ni/SiC or Ni-B. Ni-B/SiC coatings with high hardness have superior anti-wear performance. The inclusion of SiC particles into the metal or alloy matrix improved the wear resistance of the composite coatings [19]. It indicates that incorporation of 5 to 10 g L⁻¹ SiC particles in the bath can decrease the wear rate and improve the hardness of the composites. Meanwhile, the B content in the coating has great influence on the anti-wear properties.

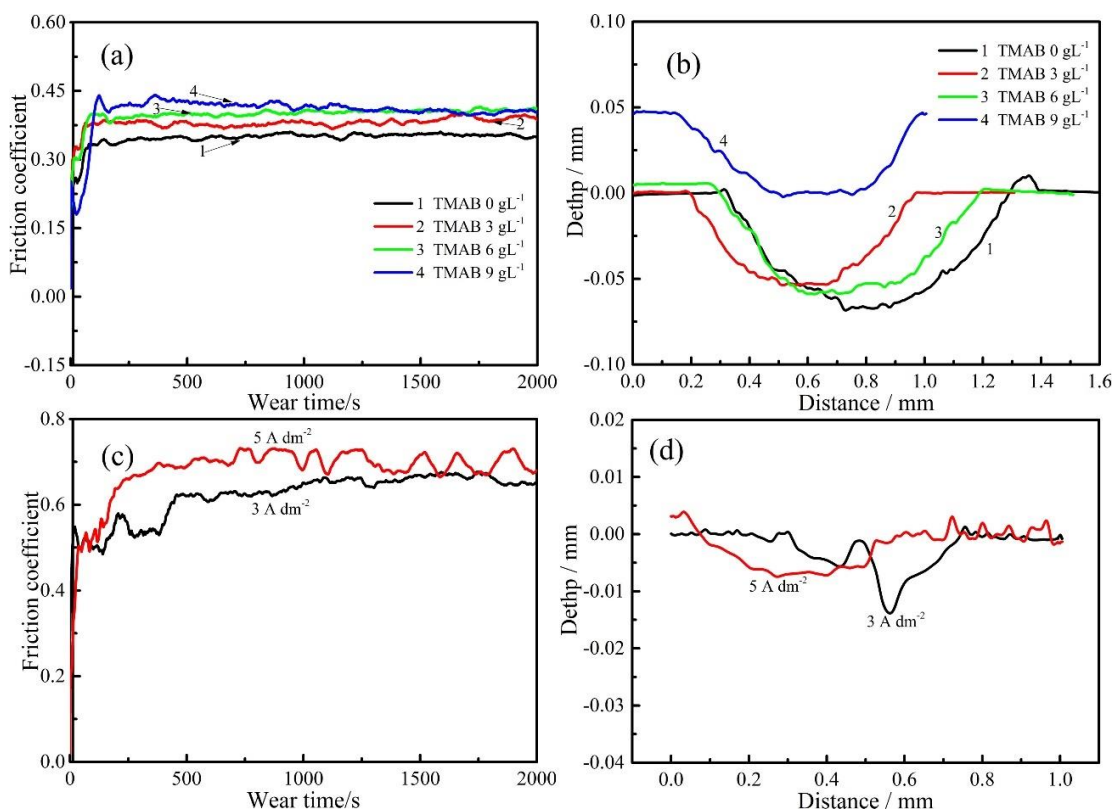


Figure 3. Friction coefficient and wear track profiles of Ni-B/SiC composite coatings electrodeposited (a, b) with different TMAB concentration; (c, d) at different current density under the dry-sliding condition (10 N, 5 Hz).

3.3 Surface electronic states of the Ni-B/SiC nanocomposite coating

The binding energies of the relative substances were analyzed by XPS to evaluate the electronic state of the Ni-B/SiC composite coatings in their as-deposited state. Fig.4 shows the XPS survey spectra of the electrodeposited coating, which shows that the peaks of Ni, B, N, C, Si, and O are displayed on the surface of the coating.

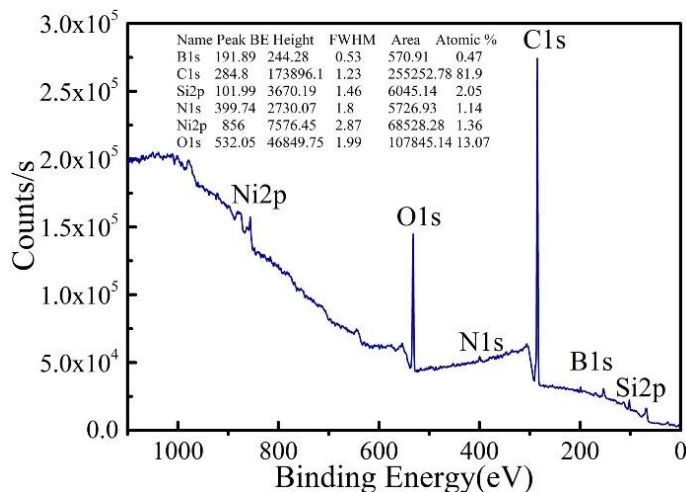


Figure 4. XPS survey spectra of the electrodeposited Ni-B/SiC composite coating.

The high-resolution XPS spectra of Ni 2p_{3/2} and B 1s are shown in Fig. 5. Fig. 5 (a) shows that the Ni 2p_{3/2} spectra can be deconvoluted into four peaks. The main peak at 853.4 eV corresponds to the metallic nickel, the peak at 855.9 eV corresponds to the NiO, and the peak at 857.3 eV corresponds to the Ni(OH)₂. The last peak at approximately 861.0 eV is assigned to the satellite peaks of complex nickel. It shows that the nickel oxidant in the bath can be reduced to metallic nickel during the electrodeposition. The binding energy values measured in the XPS spectra were in good agreement with values reported by other researchers [20, 21].

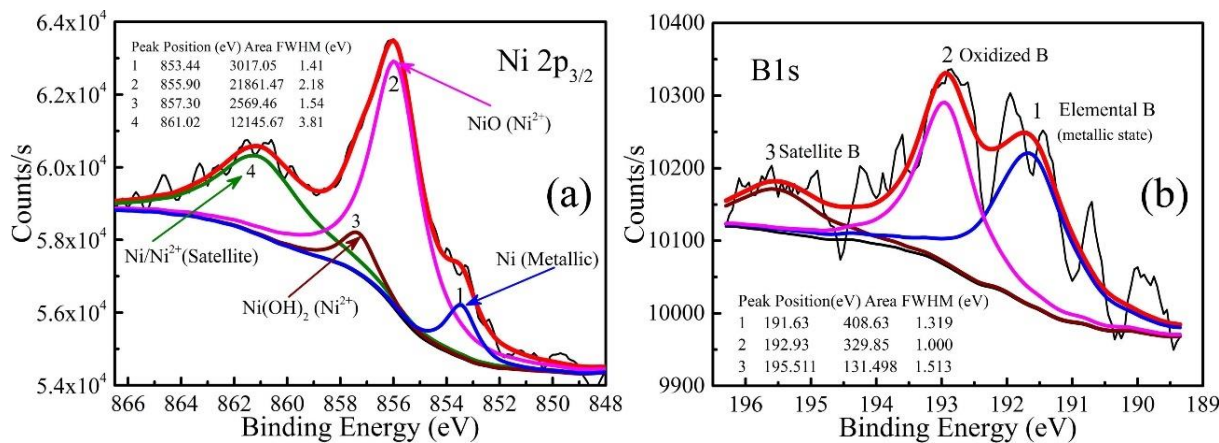


Figure 5. XPS spectra of (a) Ni 2p_{3/2} and (b) B 1s of the Ni-B/SiC composite coating in the as-deposited state.

As can be seen in Fig. 5(b), the B 1s of the as-deposited coating can be divided into three chemical states of the boron species, the peak at 191.6 eV corresponding to elemental boron. The peaks at 192.9 eV are attributed to the oxidized boron. The peaks at 195.5 eV are attributed to the satellite peak of oxidized boron. These results are consistent with previous reports [22]. Compared to the binding energy of the pure B (187.1 eV), the binding energy of elemental boron in the Ni-B/SiC positively shifts about 2.5 eV, indicating that the boron donates a partial electron to the alloying nickel. The above results could be attributed to that the bonding electrons of boron occupy vacant d-orbitals of nickel, making the B electron-deficient and the Ni metal electron-enriched. The variation of the binding energy of Ni is not as sensitive as that of B. The reason no obvious change in binding energy of elemental nickel is that the atomic weight of nickel is several times more than that of boron [23, 24].

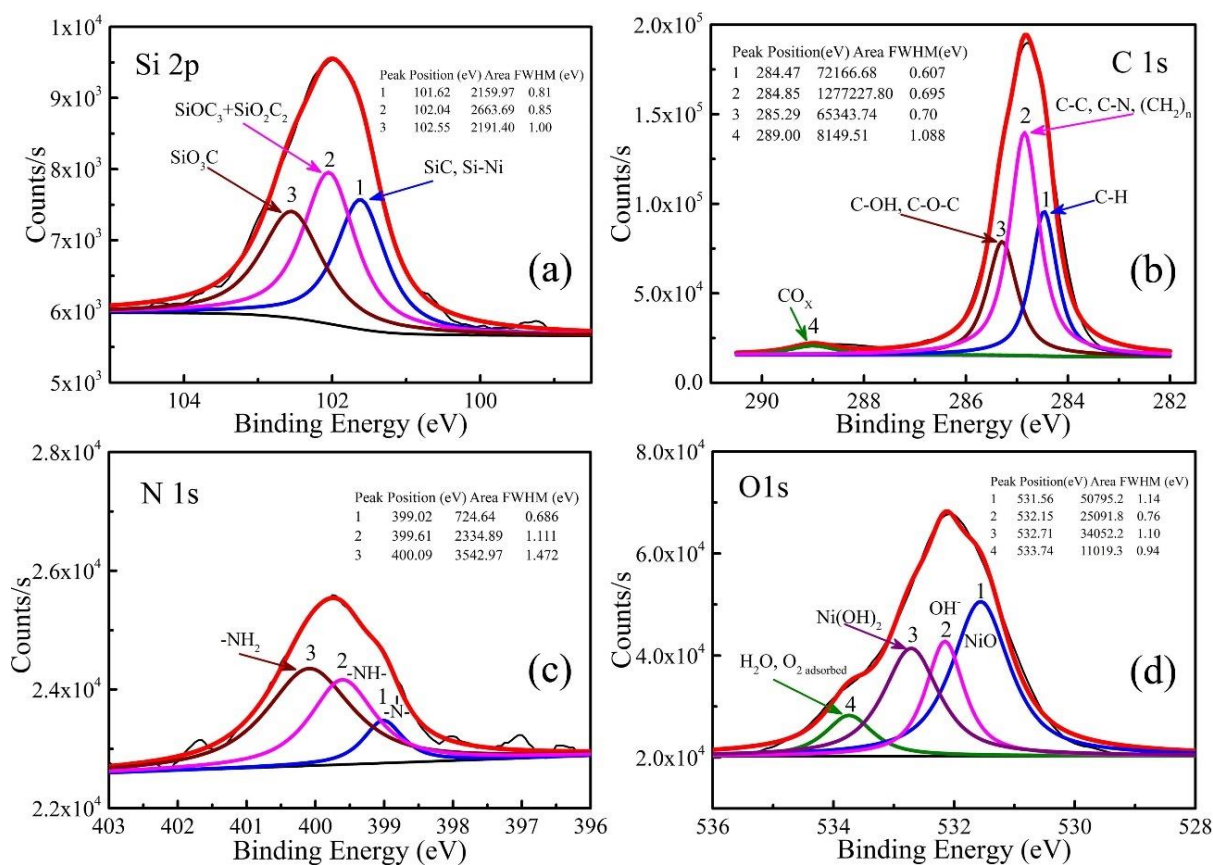


Figure 6. XPS spectra of (a) Si2p; (b) C1s; (c) N1s and (d) O1s of the Ni-B/SiC composite coating in the as-deposited state.

Fig. 6 shows the high-resolution spectra of Si 2p, C 1s, N 1s and O 1s. Fig. 6 (a) shows that the spectra of Si 2p can be separated into three peaks, the peak at 101.6 eV corresponding to the SiC, the peak at approximately 102.0 eV corresponding to the SiOC₃, and SiO₂C₂, and the peaks at approximately 102.55 eV corresponding to the SiO₃C. As shown in Fig. 6(b), the spectra of C 1s can be separated into five peaks. The peak at 284.45 eV corresponds to the C-H, the peak at 284.85 eV corresponds to the C-C, (CH₂)_n, C-N or metal-C, and the peaks at approximately 285.3 eV and 289 eV correspond to the C-OH (C-O-C) and CO_x (COOH), respectively. Obviously, C content is caused by

co-deposition of the SDS and saccharin or C contamination. The spectra of N 1s can also be split into three peaks (Fig. 6(c)). The peak at 399.0 eV corresponds to the tertiary amine (N-R₃), the peak at approximately 399.6 eV corresponds to the secondary amine (-NH-), the peaks at approximately 400.0 eV correspond to the -NH₂, or -N⁺, respectively. The high resolution of the O 1s is present in Fig. 6(d). The O 1s spectra permit separation of oxides from hydroxides. Based on the deconvolution of the O 1s spectrum, four prominent peaks were observed. They were attributed to the formation of oxides and hydroxides of Ni. The peak at 531.6 eV is attributed to the NiO. The peak at approximately 532.2 eV is associated with the OH⁻. The peak at approximately 532.7 eV is related to the Ni(OH)₂, and the last peak at approximately 533.7 eV corresponds to the H₂O or adsorbed oxygen. The presence of the OH⁻ and the O²⁻ species is responsible for the Ni(OH)₂ and NiO. The XPS analysis suggested that the as-deposited coating contains metallic nickel, oxide or hydroxide nickel, and the SiC particles. In addition, it seems that some residual bath solution appeared on the as-deposited coating surface.

4. CONCLUSIONS

In this study, Ni-B/SiC composite coating has been fabricated by electrodeposition using TMAB as boron precursor in a Ni-B electrolyte containing suspended SiC nanoparticles. The incorporation of SiC inhibits the matrix dissolution and, consequently, significantly enhances the coating corrosion resistance. In composite coatings, SiC can fill the surface defects, acting as a barrier and hindering the corrosion attack. The corrosion resistance of the Ni-B/SiC composite coating was enhanced which may be related to the dense structure, barrier effect and the reduction in the active surface area of Ni-B matrix by the inclusion of inert SiC particles. The XPS analysis suggested that the as-deposited coating contains metallic nickel, oxide or hydroxide nickel, and the SiC particles. The Ni-B/SiC coating with dense structure shows superior anti-corrosion and wear resistance than that of Ni/SiC or Ni-B, and is expected to exhibit high-performance in the marine environment.

ACKNOWLEDGEMENTS

This work was supported by the National Natural Science Foundation of China (Grant No. 51605137, 51679076 and 51301061).

References

1. J. Lapinski, D. Pletcher, F.C. Walsh, *Surf. Coat. Technol.*, 205 (2011) 5205-5209.
2. B. Li, W. Zhang, Y. Huan, J. Dong, *Surf. Coat. Technol.*, 337 (2018) 186-197.
3. B. Li, W. Zhang, W. Zhang, Y. Huan, *J. Alloys Compd.*, 702 (2017) 38-50.
4. F. Bülbül, L.E. Bülbül, *Appl. Phys. A: Mater. Sci. Process.*, 122 (2015) 25.
5. S. Eraslan, M. Ürgen, *Surf. Coat. Technol.*, 265 (2015) 46-52.
6. H. Ogihara, K. Udagawa, T. Saji, *Surf. Coat. Technol.*, 206 (2012) 2933-2940.
7. M. Romero-Romero, C. Domínguez-Ríos, R. Torres-Sánchez, A. Aguilar-Elguezabal, *Surf. Coat. Technol.*, 315 (2017) 181-187.
8. K.H. Lee, D. Chang, S.C. Kwon, *Electrochim. Acta*, 50 (2005) 4538-4543.
9. K. Krishnaveni, T.S.N. Sankara Narayanan, S.K. Seshadri, *J. Alloys Compd.*, 466 (2008) 412-420.

10. Y.N. Bekish, S.K. Poznyak, L.S. Tsybul'skaya, T.V. Gaev'skaya, *Electrochim. Acta*, 55 (2010) 2223-2231.
11. H. Ogihara, M. Safuan, T. Saji, *Surf. Coat. Technol.*, 212 (2012) 180-184.
12. H. Kwon, K. Kim, H. Ahn, Y. Kim, *Sensors and Materials*, 29 (2017) 225-234.
13. E. Correa, J.F. Mejia, J.G. Castano, F. Echeverria, M.a. Gomez, *J. Tribol.*, 139 (2017) 051302.
14. M. Ghaderi, M. Rezagholizadeh, A. Heidary, S.M. Monirvaghefi, *Prot. Met. Phys. Chem. Surf.*, 52 (2016) 854-858.
15. B. Li, W. Zhang, Y. Huan, W. zhang, *Rare Met. Mater. Eng.*, 46 (2017) 3129-3134.
16. H. Ogihara, H. Wang, T. Saji, *Appl. Surf. Sci.*, 296 (2014) 108-113.
17. E. Georgiza, V. Gouda, P. Vassiliou, *Surf. Coat. Technol.*, 325 (2017) 46-51.
18. A. Karabulut, M. Durmaz, B. Kilinc, U. Sen, S. Sen, *Acta Phys. Pol., A*, 131 (2017) 147-149.
19. B. Li, W.W. Zhang, *Int. J. Electrochem. Sci.*, 12 (2017) 7017-7030.
20. H. Li, H. Li, W. Dai, M. Qiao, *Appl. Catal., A*, 238 (2003) 119-130.
21. H. Li, H. Li, W. Dai, W. Wang, Z. Fang, J. Deng, *Appl. Surf. Sci.*, 152 (1999) 25-34.
22. I.G. Casella, M. Gatta, *Anal. Chem.*, 72 (2000) 2969-2975
23. B. Li, A. Lin, F. Gan, *Surf. Coat. Technol.*, 201 (2006) 2578-2586.
24. B. Li, A. Lin, X. Wu, Y. Zhang, F. Gan, *J. Alloys Compd.*, 453 (2008) 93-101.

© 2018 The Authors. Published by ESG (www.electrochemsci.org). This article is an open access article distributed under the terms and conditions of the Creative Commons Attribution license (<http://creativecommons.org/licenses/by/4.0/>).